

We are IntechOpen, the world's leading publisher of Open Access books Built by scientists, for scientists

4,800

Open access books available

122,000

International authors and editors

135M

Downloads

Our authors are among the

154

Countries delivered to

TOP 1%

most cited scientists

12.2%

Contributors from top 500 universities



WEB OF SCIENCE™

Selection of our books indexed in the Book Citation Index
in Web of Science™ Core Collection (BKCI)

Interested in publishing with us?
Contact book.department@intechopen.com

Numbers displayed above are based on latest data collected.

For more information visit www.intechopen.com



Web Tension and Speed Control in Roll-to-Roll Systems

Jingyang Yan and Xian Du

Abstract

Roll-to-roll (R2R) printing shows great potential for high-throughput and cost-effective production of flexible electronics, including solar cells, wearable sensors, and so on. In roll-to-roll process, precise control of the web speed and tension is critical to ensure product quality, since improper web speed and tension would lead to severe damages to the substrates. In this chapter, we will focus on the advanced control algorithms of web tension and speed control in roll-to-roll system. Two concepts of control algorithms will be presented, which are model-based control and data-based control. For model-based control algorithms, the modeling of web dynamics and an application of robust H_∞ controller will be reviewed; for data-based control algorithms, two methods of neural network control learning methods will be introduced, and the application of neural network control in web tension and speed control will be presented. Moreover, performances of different control algorithms are compared.

Keywords: roll-to-roll system, tension control, speed control, model-based control, neural network control

1. Introduction

Flexible electronics offer lightweight, thin form factor and unbreakable foldability with maximum design freedom and easy affordability, bringing the world of consumer electronics to a new age. Research works have been carried out to explore its use for a wide range of applications, from simple low-power electronic circuitry for conventional logics and mobile devices, smart and paperlike displays, efficient energy harvesting and storage capability, disposable label-free biosensors, and smart skins to autonomous wearable electronics.

In order to realize such a huge potential, appropriate mass production technologies need to be developed. The roll-to-roll (R2R) printing process as a low-cost and fast-throughput patterning, and fabrication technique on flexible substrates is the current focus. Several kinds of printing technologies, such as inkjet printing [1], microcontact printing [2], and gravure printing [3], have been successfully applied on roll-to-roll system to fabricate flexible electronics. The print resolution has achieved 50–100 nm at lab scale, which makes high-resolution flexible devices available. This high-resolution printing process requires high demands on the control of web speed and web tension, as the printed patterns would be destroyed by the fluctuation of the web speed and web tension, even the web itself may be broken or sagged. As a result, web tension and speed are two key variables that affect the quality of the manufactured products.

This chapter is aimed at introducing different methods of web tension and web speed control. The control algorithms are classified into two large groups: model-based control and data-based control. For model-based control, first, the dynamic model of the web handling system is developed. After that, two major control algorithms, PID and decentralized control, are presented. For data-based control, the application of neural network control will be discussed. Moreover, performances of the above control algorithms are compared.

2. Model-based control

Model-based control mentioned here refers to plant modeling based on physical laws. The mathematical model conceived is used to identify dynamic characteristics of the plant model. Controllers can be synthesized based on these characteristics. The main steps in model-based method are:

1. Plant modeling. Plant modeling is based on physical laws, where a model consists in connected blocks that represent the real physical elements of the plant. Usually, certain parameters are hard to measure, such as the model of load cells and motors in roll-to-roll system. In this situation, parameter optimization could be applied. It is done in several steps in order to reduce the number of parameters to identify at each step.
2. Controller analysis and synthesis. Based on the model of the plant, differential-algebraic equations can be derived which governs plant dynamics. Different control algorithms can then be designed.

In this section, the modeling of roll-to-roll web handling system is derived. A robust H_∞ controller is then introduced. This work is mainly from Refs. [4-6].

2.1 Dynamic model

A typical roll-to-roll system can be divided into two parts: web handling part and printing part. Here, we will focus on the web handling part. Web handling refers to the physical mechanics related to the transport and control of web materials through processing machinery. It is common to divide a process line into several tension zones by denoting the span between two successive driven rollers as a tension zone in web handling. Since the free roller dynamics influences the web tension only during the transients due to acceleration/deceleration of the web line and negligible effect during steady-state operation, the assumption that the free rollers do not contribute to web dynamics during static operation is reasonable. This assumption will be used in developing dynamic model. Also it is assumed that there is no slip between the web and rollers, and the web is elastic.

Figure 1 shows a web line with three tension zones. It consists of four motorized rollers and three load cells. Load cells are mounted between each pair of rollers which are used to measure the web tension. The driving motors are denoted by M_i for $i = 0, 1, 2,$ and 3 , u_i denotes input torque from the i th motor, v_i represents the linear web speed on the i th roller, and t_i represents the web tension in the span between $(i - 1)$ th and i th rollers. There are four sections in the web line in **Figure 1**, which are the unwind section, master speed roller, process section, and rewind section. Master speed roll is used to set the reference speed of the whole web process lines. The unwind roll and rewind roll release/accumulate material to/from the processing

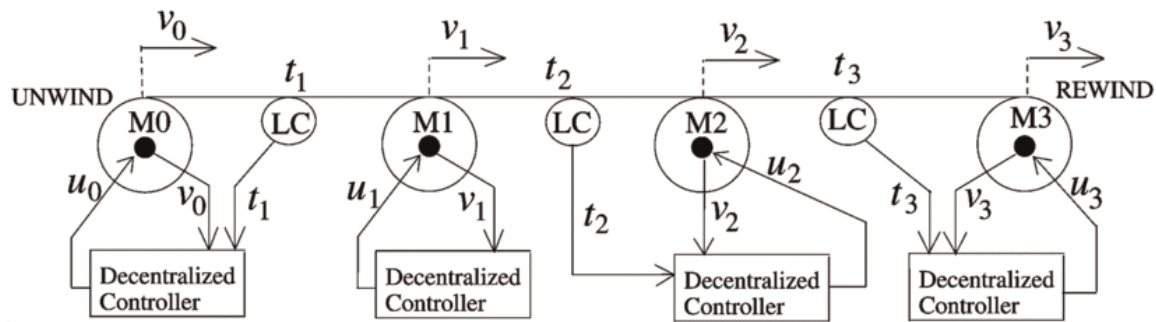


Figure 1.
 A web processing line with four motorized rolls and three load cells.

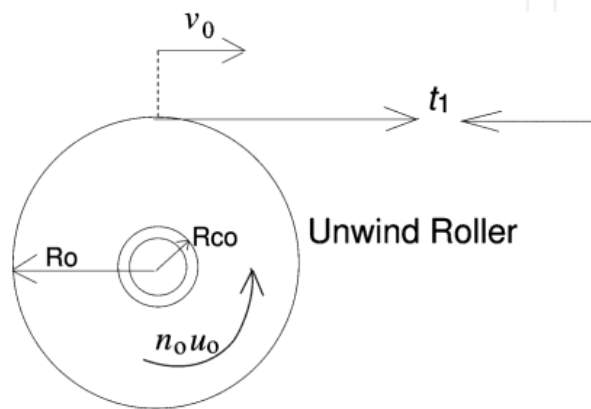


Figure 2.
 Model of unwind roll for dynamic analysis.

section of the web line. Thus, their radius and inertia are time-varying. The dynamics of different sections are introduced in the following.

Unwind section: A cross-sectional view of the unwind roll is shown in **Figure 2**. The associated local state variables for the unwind section are web speed v_0 and tension t_1 . At any time t , the effective inertia $J_0(t)$ of the unwind roller is given by

$$J_0(t) = n_0^2 J_{m0} + J_{c0} + J_{w0}(t) \quad (1)$$

where n_0 is the gearing ratio between the motor shaft and unwind roll shaft. J_{m0} is the inertia of all the rotating parts on the motor side, which includes inertia of motor armature, driving pulley, deriving shaft, etc. J_{c0} is the inertia of the driven shaft and the core mounted on it. J_{w0} is the inertia of the cylindrical wound web material on the core. Both J_{m0} and J_{c0} are constant, but J_{w0} is not constant due to the releasing the web. The inertia, J_{w0} , is given by

$$J_{w0}(t) = \frac{\pi}{2} b_w \rho_w (R_0^4(t) - R_{c0}^4) \quad (2)$$

where b_w is the width, ρ_w is the density of the web material, R_{c0} is the radius of the empty core, and $R_0(t)$ is the radius of the material roll.

The speed dynamics of the unwind roll can be written as

$$\frac{d}{dt}(J_0 \omega_0) = t_1 R_0 - n_0 u_0 - b_{f0} \omega_0 \quad (3)$$

$$\dot{J}_0 \omega_0 + \dot{\omega}_0 = t_1 R_0 - n_0 u_0 - b_{f0} \omega_0 \quad (4)$$

where ω_0 is the angular speed of the unwind roll and b_{f0} is the coefficient of friction in the unwind roll shaft. The change rate in J_0 is only because of the change in $J_{\omega_0}(t)$, and from Eq. (2), the rate of change of $J_0(t)$ is given by

$$\dot{J}_0(t) = \dot{J}_{\omega_0}(t) = 2\pi b_{\omega} \rho_{\omega} R_0^3 \dot{R}_0 \quad (5)$$

The speed of the web coming off the unwind roll is related to the angular speed of the unwind roll by $v_0 = R_0 \omega_0$. Hence, ω_0 can be obtained in terms of v_0 as

$$\dot{\omega}_0 = \frac{\dot{v}_0}{R_0} - \frac{\dot{R}_0 v_0}{R_0^2} \quad (6)$$

Substitute Eqs. (4) and (5) into Eq. (3), we have

$$\frac{J_0}{R_0} \dot{v}_0 = t_1 R_0 - n_0 u_0 - \frac{b_{f0}}{R_0} v_0 + \frac{\dot{R}_0 v_0}{R_0^2} J_0 - 2\pi \rho_{\omega} b_{\omega} R_0^2 \dot{R}_0 v_0 \quad (7)$$

The rate of change of radius, R_0 , is a function of the speed v_0 and the web thickness t_w and is approximately given by

$$\dot{R}_0 \approx -\frac{t_w v_0(t)}{2\pi R_0(t)} \quad (8)$$

This is because the thickness affects the rate of change of the radius of the roll only after each revolution of the roll; the continuous approximation is valid since the thickness is generally very small. Hence, Eq. (6) can be simplified to

$$\frac{J_0}{R_0} \dot{v}_0 = t_1 R_0 - n_0 u_0 - \frac{b_{f0}}{R_0} v_0 - \frac{t_w}{2\pi R_0} \left(\frac{J_0}{R_0} - 2\pi \rho_{\omega} b_{\omega} R_0^2 \right) v_0^2 \quad (9)$$

To derive the dynamic behavior of the web tension as shown in **Figure 3**, we need three laws:

Hooke's law, which models the elasticity of the web

Coulomb's law, which gives the web tension variation due to the friction and to the contact force between web and roll

Mass conservation law, which expresses the cross-coupling between web velocity and web strain

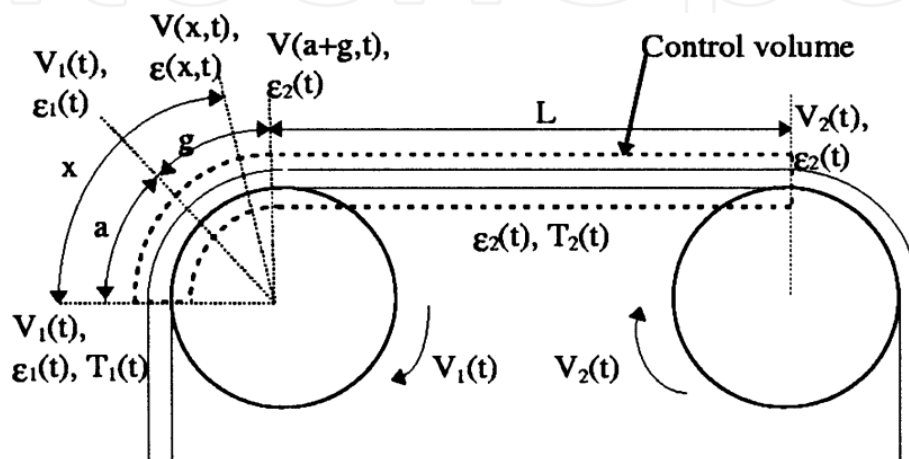


Figure 3. Model for calculating web tension.

For Hooke's law, the tension t of an elastic web is the function of the web strain ε :

$$T = ES\varepsilon = ES \frac{L - L_0}{L_0} \quad (10)$$

where E is Young's modulus, S is the web section, L is the web length under stress, and L_0 is the nominal web length. Note that Hooke's law is valid for most web materials, if the tension is not too large. Moreover, the Young's modulus is very sensitive to the temperature and the humidity level. On the processing line, the web may go through different processes. Therefore, its elasticity properties may considerably change during the process.

Coulomb's law: The study of the web tension on a roll can be considered as a problem of friction between solids. On the roll, the web tension is constant on a sticking zone which is an arc of length a and varies on a sliding zone which is an arc of length g . Then, the web strain between the first contact point of a roll and the first contact point of the flowing roll is given by

$$\varepsilon(x, t) = \begin{cases} \varepsilon_1(t) & x \leq a \\ \varepsilon_1(t)e^{\mu(x-a)} & a \leq x \leq a + g \\ \varepsilon_2(t) & a + g \leq x \leq L_t \end{cases} \quad (11)$$

where μ is the friction coefficient and $L_t = a + g + l$.

The tension change occurs on the sliding zone, while the web speed is equal to the roll speed on the sticking zone. A sliding zone can also appear at the roll entry if the tension varies at high rate.

Mass conservation law: Consider a web of length $L = L_0(1 + \varepsilon)$ with weight density ρ , under a unidirectional stress. If the cross section stays constant, then, according to the mass conservation law, the mass of the web remains constant between the state without stress and the state under stress

$$\rho SL = \rho_0 SL_0 \Rightarrow \frac{\rho}{\rho_0} = \frac{1}{1 + \varepsilon} \quad (12)$$

Based on these three laws, web tension between two successive rolls can be obtained. The equation of continuity applied to the web transport system gives

$$\frac{\partial \rho}{\partial t} + \frac{\partial(\rho V)}{\partial x} = 0 \quad (13)$$

where V represents the web speed in the control volume. Using Eq. (12), we integrate on the control volume V defined by the first contact points between the web and the rolls:

$$\int_V \frac{\partial}{\partial t} \left(\frac{1}{1 + \varepsilon} \right) dV = - \int_V \frac{\partial}{\partial x} \left(\frac{V}{1 + \varepsilon} \right) dV \quad (14)$$

If the web section is constant, $dV = Sdx$, we can integrate with respect the variable x from 0 to L_t :

$$\frac{\partial}{\partial t} \left(\int_0^{L_t} \frac{1}{1 + \varepsilon(x, t)} dx \right) = - \int_0^{L_t} \frac{\partial}{\partial x} \left(\frac{V(x, t)}{1 + \varepsilon(x, t)} \right) dx \quad (15)$$

Using Eq. (11) and assuming that $a + g \ll L$, we can obtain

$$\int_0^{L_t} \frac{1}{1 + \varepsilon(x, t)} dx \approx \frac{L}{1 + \varepsilon(L_t, t)} \quad (16)$$

Let $\varepsilon(0, t) = \varepsilon_1$, $\varepsilon(L_t, t) = \varepsilon_2$, $V(0, t) = V_1$ and $V(L_t, t) = V_2$; then, the final relationship is

$$\frac{d}{dt} \left(\frac{L}{1 + \varepsilon_2} \right) = \frac{V_1}{1 + \varepsilon_1} - \frac{V_2}{1 + \varepsilon_2} \quad (17)$$

Assuming that $\varepsilon_1 \ll 1$, $\varepsilon_2 \ll 1$, then

$$\frac{1}{1 + \varepsilon} \approx 1 - \varepsilon \quad (18)$$

Considerable mathematical simplification can be obtained by using Eqs. (18) in (17) as follows:

$$L \frac{d}{dt} (1 - \varepsilon_2) = (1 - \varepsilon_1)V_1 - (1 - \varepsilon_2)V_2 \quad (19)$$

Rearranging equation and using Eq. (1) gives

$$L \frac{dT_2}{dt} = AE(V_2 - V_1) + T_1V_1 - T_2V_2 \quad (20)$$

Hence, dynamic behavior of the web tension t_1 is given by

$$L_1 \dot{t}_1 = AE[v_1 - v_0] + t_0v_0 - t_1v_1 \quad (21)$$

Master speed roller: The dynamics of the master speed roller are given by

$$\frac{J_1}{R_1} \dot{v}_1 = (t_2 - t_1)R_1 + n_1u_1 - \frac{b_{f1}}{R_1}v_1 \quad (22)$$

Processing section: The web tension and web velocity dynamics in the process section are given by

$$L_2 \dot{t}_2 = AE[v_2 - v_1] + t_1v_1 - t_2v_2 \quad (23)$$

$$\frac{J_2}{R_2} \dot{v}_2 = (t_3 - t_2)R_2 + n_2u_2 - \frac{b_{f2}}{R_2}v_2 \quad (24)$$

Sometimes there are idler rolls in processing section; in that case, we can ignore the torque generated by the motor in Eq. (24).

Rewind section: The web dynamics of speed in rewinding section are similar to those in unwind section, and the only difference is that the radius of rewind roll is increasing. The web tension and speed dynamics in rewind section are

$$L_3 \dot{t}_3 = AE[v_3 - v_2] + t_2v_2 - t_3v_3 \quad (25)$$

$$\frac{J_3}{R_3} \dot{v}_3 = -t_3R_3 + n_3u_3 - \frac{b_{f3}}{R_3}v_3 + \frac{t_\omega}{2\pi R_3} \left(\frac{J_3}{R_3^2} - 2\pi\rho_\omega b_\omega R_3^2 \right) v_3^2 \quad (26)$$

Equations (9) and (21)–(26) represent the dynamics of the web handling. Extension to other web lines can be easily made based on this model. However, it is necessary to emphasize all the assumptions when using this model:

1. The length of contact region between the web material and a roller is negligible compared to the length of free web span between the rollers (i.e., the strain variations in the contact region are negligible).
2. The thickness of the web is very small compared with the radius of rollers over where the web is wrapped.
3. There is no slippage between the web material and the rollers.
4. There is no mass transfer between the web material and the environment (i.e., no humidification or evaporation).
5. The strain in the web is small (much less than unity).
6. The strain is uniform within the web span.
7. The web cross section in the unstretched state does not vary along the web.
8. The density and the modulus of elasticity of the web in the unstretched state are constant over the cross section.
9. The web is perfectly elastic.
10. The web material is isotropic.
11. The web properties do not change with temperature or humidity.

2.2 Model-based robust H_∞ control

To synthesize the controllers, we need a linearized model of the plant. The linear model is obtained by linearizing the simplified form of the equations around the nominal web tension and velocity, by assuming slow variations of the radius and inertia. Let $T = t - t_0$, $V = v - v_0$, where t_0 and v_0 are tension and speed reference and T and V are the variants in tension and speed, respectively. At the initial steady-state operating condition, the equation must be satisfied:

$$0 = -v_{10} + v_{20} + \epsilon_{10}v_{10} - \epsilon_{20}v_{20} \quad (27)$$

The following linearized model results from applying Eq. (27) with Eq. (21), and dropping second-order terms:

$$L_i \dot{t}_i = AE[v_i - v_{i-1}] + v_0(t_{i-1} - t_i) \quad (28)$$

Using Eqs. (14), (22), (24), (26), and (28), the state-space representation of the nominal model around an operation point, $V_i = V_0$, for $i = 1, 2, 3, 4, 5$, $T_i = T_0$ for $i = 2, 3, 4, 5$, with a web tension on the unwound roller equal to zero can be expressed as

$$\begin{aligned} E_m \dot{X} &= A(t)X + BU \\ Y &= CX \end{aligned} \quad (29)$$

Here, model Eq. (29) is called nominal model G_0 of the web handling system.

Robust H_∞ control is a powerful tool to synthesize multivariable controllers with interesting properties of robustness and disturbance rejection. The robust controller is designed according to nominal model G_0 with full unwind roller and empty rewind roller. The robust H_∞ controller is synthesized using the mixed sensitivity approach [7, 8], as shown in **Figure 4**, where w is the exogenous inputs and z is the controlled signals.

The frequency-weighting functions W_p , W_u , and W_t appear in the closed-loop transfer function matrix in the following manner:

$$T_{wz} := \begin{bmatrix} W_p S \\ W_u K S \\ W_t T \end{bmatrix} \quad (30)$$

where S is the sensitivity function, $S = (1 + GK)^{-1}$, and T is the complementary sensitivity function $T = I - S$.

The controller K is calculated using “ γ -iterations” [9]. It is a stabilizing controller such that the H_∞ norm of the transfer function between w and z is

$$\|T_{wz}\|_\infty := \sup_w \sigma_{\max}(T_{wz}(j\omega)) \leq \gamma \quad (31)$$

With γ close to γ_{\min} , the smallest possible value of γ . In a sense, the controller K “minimizes” the transfer between w and the controlled signal z .

The frequency-weighting function W_p is usually selected with a high gain at low frequency to reject low-frequency perturbations and to reduce steady-state error. The structure of W_p is as follows:

$$W_p(s) = \frac{\frac{s}{M} + w_B}{s + w_B \varepsilon_0} \quad (32)$$

where M is the maximum peak magnitude of S , $\|S\|_\infty \leq M$, w_B is the required bandwidth frequency, and ε_0 is the steady-state error allowed. The weighting function W_u is used to avoid large control signals, and the weighting function W_t increases the roll-off at high frequency. **Figure 5** shows the performances of PID controller and multivariable H_∞ robust control.

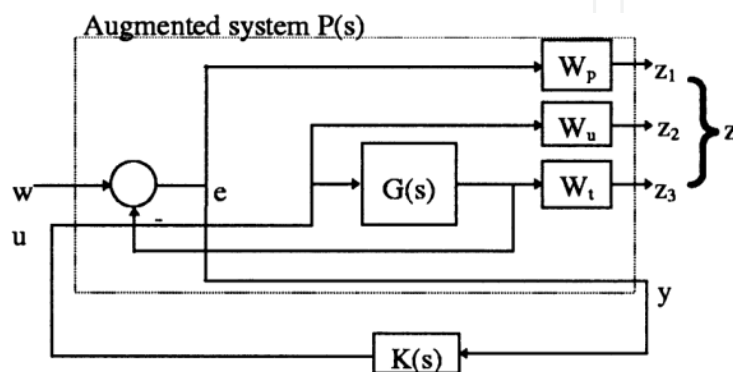


Figure 4. Mixed sensitivity method for H_∞ controller design.

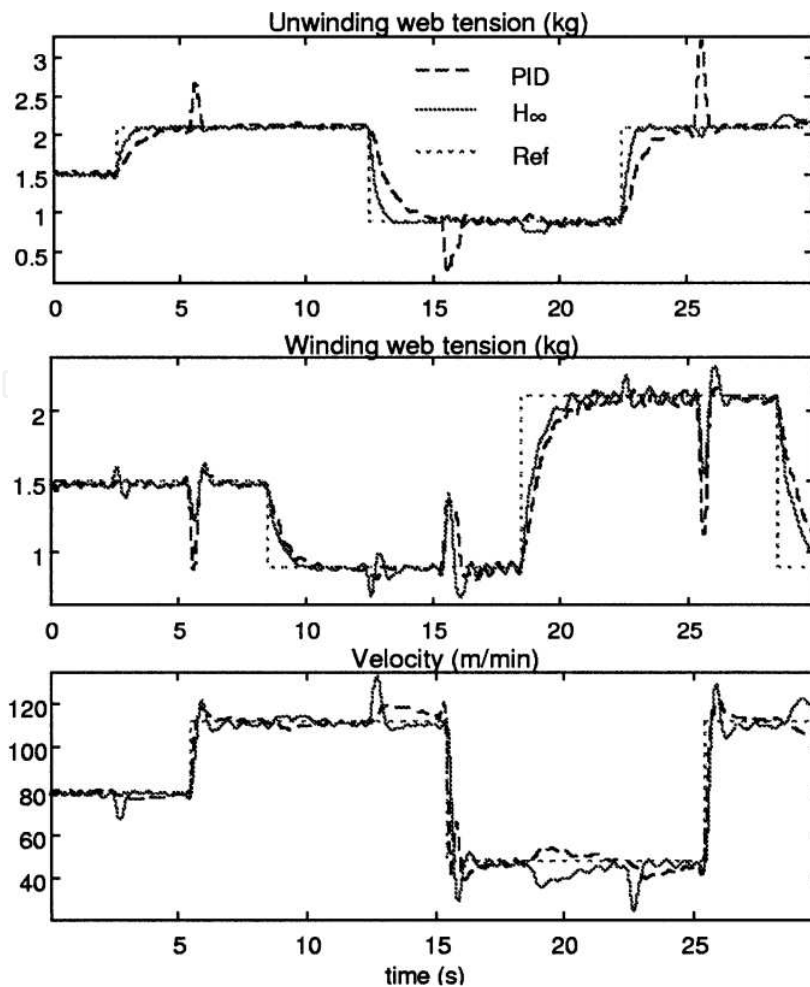


Figure 5.
Performances of robust H_{∞} controller and PID controller.

3. Data-based control

From the physical model of the web handling part, we can see that the model is nonlinear and time-variant, which leads to difficulties in monitoring the dynamics. Besides, in order to implement controllers, the model is linearized by dropping the high-order terms. Thus, the designed controller can't follow closely enough the dynamics of the system during all the winding process. Moreover, up to 11 assumptions are made to derive the model. However, we can't guarantee that all the assumptions are satisfied, which may cause a large difference between the performance of the model and the real plant. To overcome these disadvantages of model-based control, data-based control was carried out. In data-based control, the identification of the plant model and/or the design of the controller are based entirely on experimental data collected from the plant. The controlled plants in data-based control are treated as black-boxes, which the dynamics of plants can be learned using a large amount of sensory data.

The standard approach in data-based control system design has two steps:

1. Model identification: The basic idea of data-based control is to make use of the wealth of data obtained from sensors to learn the dynamics of the plant. These data are also called training data.

2. Controller design: The controller design could be done in the same way as in model-based control, such as neural generalized predictive control (GPC). Meanwhile, training method can also be applied for training the controller, like neural network control.

In this section, we will introduce an application of one data-based control algorithm, i.e., neural network control, in web tension and speed control of roll-to-roll system.

3.1 Neural network

Neural network is a universal approximator, which is capable of approximating any measurable function to any desired degree of accuracy. Hence, we could use neural network to learn the dynamics of plants. Here, we use the classical definition of neural network in Ref. [10]. Neural network consists of networks of artificial neurons in which the data flows through and their weights are changed to reduce the error in the learning process. A one-layer neural network is typically presented by a network diagram as in **Figure 6**. Derived features Z_m are created from linear combinations of the inputs; then the output Y is modeled as a function of linear combinations of the Z_m :

$$\begin{aligned} Z_m &= \sigma(\alpha_{0m} + \alpha_m^T X), \quad m = 1, \dots, M \\ T_k &= \beta_{0k} + \beta_k^T Z, \quad k = 1, \dots, K \\ f_k(X) &= g_k(T), \quad k = 1, \dots, K \end{aligned} \quad (33)$$

The activation function $\sigma(v)$ is usually chosen to be the sigmoid:

$$\sigma(v) = \frac{1}{1 + e^{-v}} \quad (34)$$

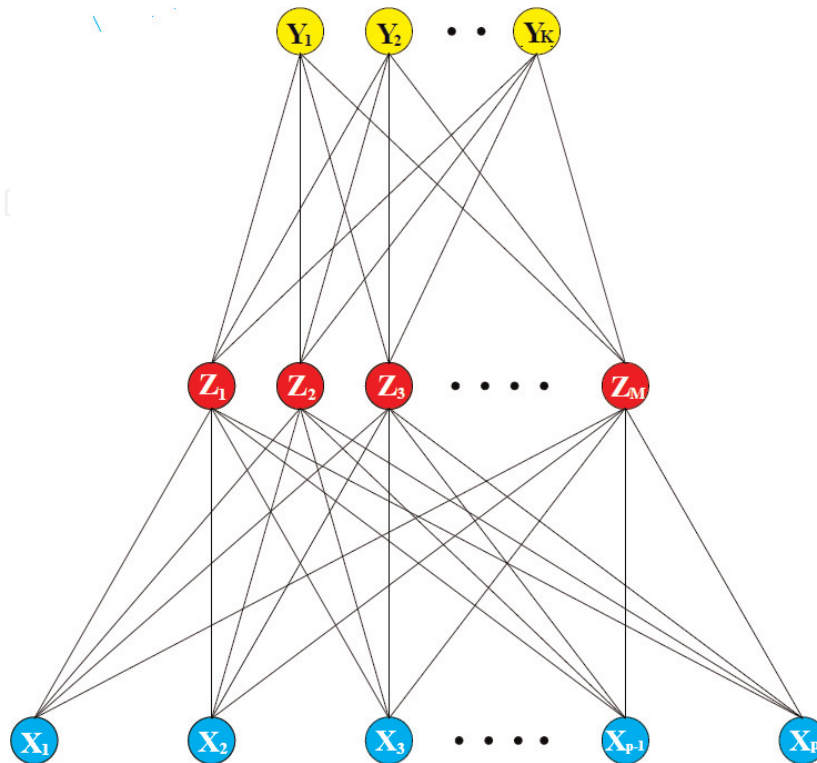


Figure 6. Schematic of a single-layer feedforward neural network.

β and α are additional bias feeding into every unit in the hidden and output layers, which captures the intercepts of α_{0m} and β_{0k} in model.

For output function $g_k(T)$, we usually choose the identity function $g_k(T) = T$.

The units in the middle of the network are called hidden units as the values Z_m are not observed directly. Generally, there can be more than one hidden layer.

ANN encompasses various types of learning algorithms, the most popular of which include feedforward neural network and recurrent neural network.

In feedforward neural network, the data flow is one directional, which is from the input layer through hidden layers to the output layer without loop and feedback.

In recurrent neural network, some of the outputs are fed back to the input layer. One of the applications of recurrent neural network is time series prediction, which then can be applied in predictive control [11].

After a certain neural network is built, it needs to get training, which is to find a set of weights to minimize the error between the real outputs and predicted outputs. Backpropagation is a method used in neural networks to calculate a gradient that is need in the calculation of the desired weights based on mean squared error loss function [12]. This method has two steps: first data are fed into the network from input layer, and the activations for each layer of neurons are cascaded forward; then based on the loss, we calculate the gradient from the output layer to the input layer and update the weights.

3.2 Neural network control

In control system, in order to implement an effective algorithmic controller, we must have a thorough understanding of the plant that is to be controlled, which is very difficult in practice. A neural network controller performs a specific form of adaptive control, as it has nonlinear network and adaptable parameters. The learning process gradually tunes the weights so that the errors between the desired outputs and actual plant outputs are minimized. Here we introduce two learning structures to minimize the error signal, which are both simple and easy to understand and implement [13].

Figure 7 shows the general learning method for training the neural network controller that does minimize the overall error. The training sequence is as follows. A plant input u is applied to the plant to get a corresponding y . The network is trained to reproduce u at its output from y . Then the trained neural network controller should be able to reproduce an appropriate input u based on the desired output d . This will certainly work if the desired output d is sufficiently close to one of the training data y . Thus, the success of this method highly relies on the ability of the neural network to learn to respond correctly to inputs that are not applied in the

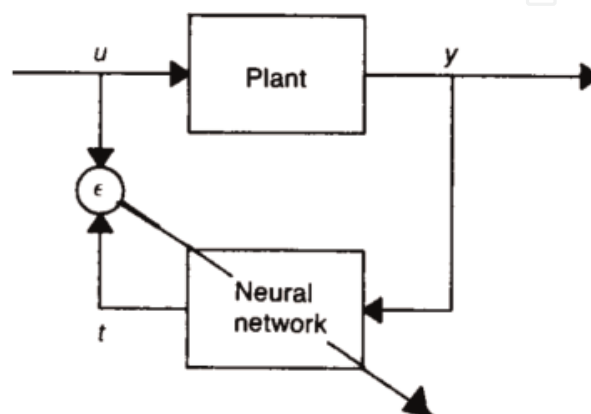


Figure 7.
Generalized learning structure.

training phase. Notice that we can't select the training data in regions of interest as we don't know which plant inputs correspond to the desired outputs d . Thus, we typically try to uniformly populate the input space of the plant with training data so that the neural network can interpolate the intermediate region. In this case, the general learning method may have to learn a larger operational range than is necessary which is time consuming.

Figure 8 shows the specialized learning method for training the neural network controller to operate properly in regions of interest only. The desired output d is used as the input to the network. The neural network is training to find the input u that derives the system output y to the desired d . The training is accomplished by using the error between the desired d and actual plant output to adjust the weights using gradient decent procedure; during each iteration the weights are adjusted to reduce the error. Notice that this procedure needs knowledge of the Jacobian of the plant. This method can be learned in the region of specialization and can be trained online. However, the general method must be trained offline. Feedforward neural networks are nondynamical systems and, therefore, input-output stable. Consequently, offline training presents no stability problem for the control system. Intuitively, we expect no stability problem in offline training, if we add penalty to the weights in loss function and the learning rate is slower enough.

3.3 Neural network control application in web tension and speed control

Figure 9 presents the prototype of our roll-to-roll system. Here, we only use the web handling part to test the neural network controller. The web handling part consists of one unwind roll, one rewind roll, one idler roll, and one tension-measuring roll. The web unwinds at unwinder and passes through the idler roll and tension-measuring roll and rewinds at rewind roll. A ring encoder and a readhead (RENISHAW MF100F and LM10) are mounted on the idler roll, which the diameter is 3 inches, to measure the linear web moving speed with a resolution of 1,310,720 CPR. The tension-measuring roll (FMS RMG1922) is used to measure the tension of the web with 1 kHz sampling rate and 0.25 N resolution. The unwind roll and rewind roll are driven by two servo motors (YASKAWA SIGMA-7). The rewind roll is used to control the web speed according to the measured speed from the encoder. The unwind roll is used to control the tension based on the feedback signals from the tension-measuring roll. The diameter of unwind roll and unwind roll are both 3.25 inches after installing the core. The web we used here is MYLAR type A film with 5 mil thickness and 4 inches width.

The data acquisition, A/D conversion, data processing, and control algorithm are all carried out using NI CompactRIO (NI CompactRIO 9049). The motor control is done by LabVIEW SoftMotion Module. The integrated field-programmable gate

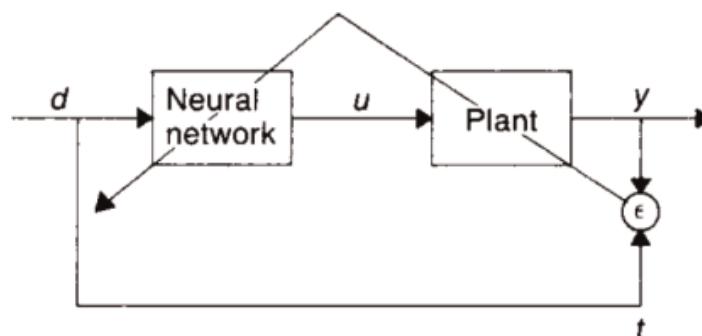


Figure 8.
Specialized learning structure.

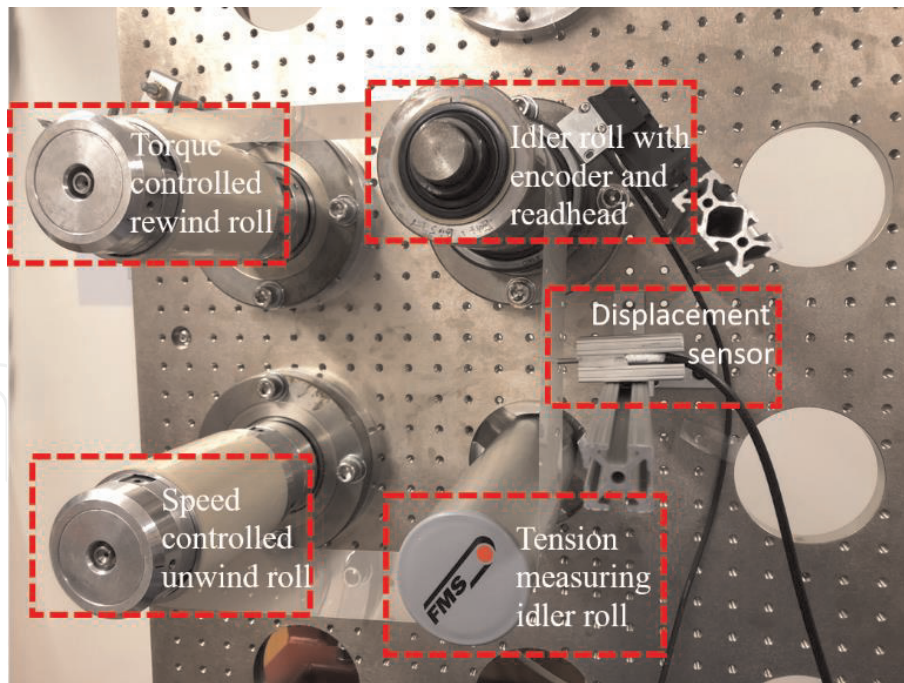


Figure 9.
 Experimental setup of web handling system.

array (FPGA) in CompactRIO is used to receive the encoder signals and tension signals with up to 40 MHz sampling rate.

A single-layer feedforward neural network with time-delayed structure is generated to learn the plant using generalized learning method. The structure is shown in **Figure 10**. The inputs to this network consist of external inputs, $u(t)$ and $y(t-1)$, and their corresponding delay nodes, $u(t-1), \dots, u(t-d_u)$ and $y(t-2), \dots, y(t-d_y)$. The parameters d_u and d_y represent the number of delay nodes. The advantage of this time-delayed structure is to help the neural network to learn the dynamics of the plant with time-variant parameters. As mentioned above, the disadvantage of generalized learning method is that we need to train the model in a large region. To overcome it, we demonstrate a simple method to find the possible region of interest. We first applied an untuned PID controller to the system. The input to the PID controller is the desired tension or speed. Then we recorded the outputs of the PID controller, which are the real inputs to the plant and the real outputs of the plant. These data are fed into the neural network. Here, we set the time delay d_u and d_y to 8 and the size of hidden layers here is 10; the activation function is *tansig* for the hidden layer and *purelin* for output layer.

The building and training of the neural network are both done in MATLAB. In Ref. [14], the trained neural network is called in LabVIEW through MATLAB

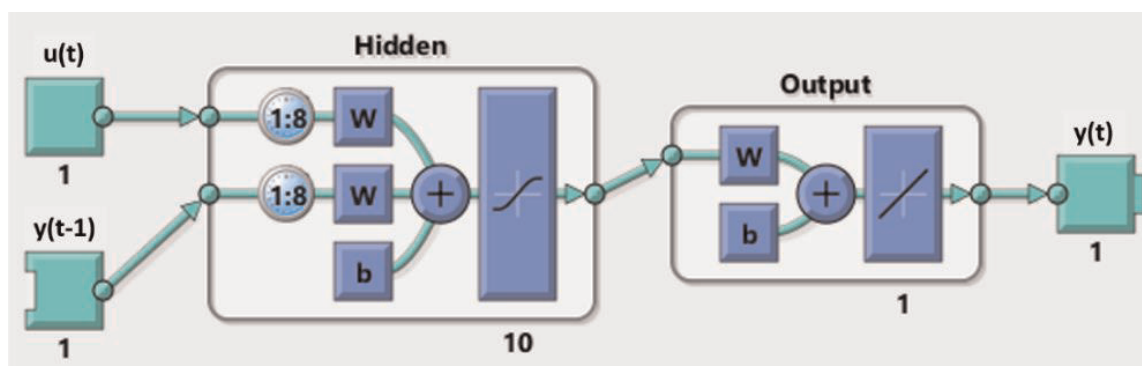


Figure 10.
 The structure of neural network for controller.

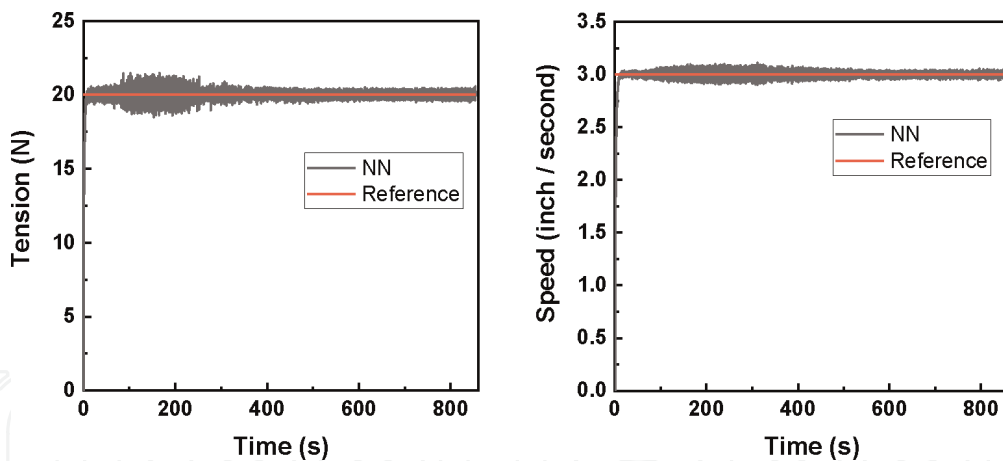


Figure 11.

Results of neural network control of web tension and speed. The left figure shows the tension performance and the right figure shows the speed performance.

scripts. However, we find that this implementation would consume a rather long time, which is about 100 ms in our application. Since this delay is caused by the communication between MATLAB program in personal computer and LabVIEW program in NI CompactRIO, if we put the neural network into the CompactRIO directly, the delay could be eliminated entirely. Therefore, we compiled the MATLAB code into a shared objects file (.so) which can be integrated to CompactRIO directly. The resulted time to call the neural network is reduced to 20 μ m, which is fast enough for real-time application.

Figure 11 shows the results of using neural network to control web speed and tension. The reference speed and tension are set to 3 inch/second and 20 N, respectively. We have recorded the web tension and speed during the whole process. The maximum deviation ($\Delta T/T$) of measured tension is 7 and 4% for speed ($\Delta V/V$). The standard deviation is 0.2% for tension and 0.1% for speed. The tension requirement in roll-to-roll fabrication is error within 10%. Thus, the neural network controller meets the requirements. Moreover, using neural network to control web speed and tension saves lots of work and time in identifying the mathematical model of roll-to-roll system. We should mention that, during the starting phase, the variation of speed and tension is both larger than the other phases. The possible reason is that the training data from PID controller doesn't cover the region of interest in this phase, so that the interpolation of neural network is not accurate. Our future work will include investigating this issue.

4. Conclusion

Roll-to-roll fabrication is known as a cost-effective method in producing electronic devices on flexible substrates. However, improper tension and speed may cause manufacturing defects of the substrate, including web wrinkling, edge cracks, and web misalignment, which lead to damages and wastes of the products. Hence, the study and control of web handling systems are carried out for decades. In this chapter, we introduce the two set of control algorithms in web handling field, model-based control and data-based control. In model-based control, a mathematical model of web tension and speed is derived. Based on the model, a robust H controller is applied. In data-based model, neural network control is discussed in detail. Two major learning methods are compared. A real application of neural network control in web handling is realized in roll-to-roll system. Both control algorithms have advantages and disadvantages. For model-based control, the

physical laws behind the dynamics of plant are clear; however, certain parameters of the model are difficult to identify, and some control algorithms are hard to realize in real life. For data-based control, the design of the controllers is simple and easy to implement, but we don't know what happens inside the controller. Consequently, it is worth to explore different control algorithms for a certain roll-to-roll system and then choose the one with the best performance.

Acknowledgements

We also thank Mehdi Riza, Neel Prakashchandra, Mehta Jonathan Lombardi, and Patrick Caviston for their help in the setup of the roll-to-roll machine.

Conflict of interest


The authors declared that they have no conflicts of interest to this work.

Author details

Jingyang Yan and Xian Du*
Department of Mechanical and Industrial Engineering, University of
Massachusetts, Amherst, MA, USA

*Address all correspondence to: xiandu@umass.edu

IntechOpen

© 2020 The Author(s). Licensee IntechOpen. This chapter is distributed under the terms of the Creative Commons Attribution License (<http://creativecommons.org/licenses/by/3.0>), which permits unrestricted use, distribution, and reproduction in any medium, provided the original work is properly cited. 

References

- [1] Siringhaus H, Kawase T, Friend R, Shimoda T, Inbasekaran M, Wu W, et al. High-resolution inkjet printing of all-polymer transistor circuits. *Science*. 2000;**290**(5499):2123-2126
- [2] Perl A, Reinhoudt DN, Huskens J. Microcontact printing: Limitations and achievements. *Advanced Materials*. 2009;**21**(22):2257-2268
- [3] Noh J, Yeom D, Lim C, Cha H, Han J, Kim J, et al. Scalability of roll-to-roll gravure-printed electrodes on plastic foils. *IEEE Transactions on Electronics Packaging Manufacturing*. 2010;**33**(4):275-283
- [4] Pagilla PR, Siraskar NB, Dwivedula RV. Decentralized control of web processing lines. *IEEE Transactions on Control Systems Technology*. 2007;**15**(1):106-117
- [5] Koc H, Knittel D, De Mathelin M, Abba G. Modeling and robust control of winding systems for elastic webs. *IEEE Transactions on Control Systems Technology*. 2002;**10**(2):197-208
- [6] Shin KH. Distributed Control of Tension in Multi-Span Web Transport Systems [thesis]. Stillwater: Oklahoma State University; 1991
- [7] Skogestad S, Postlethwaite I. *Multivariable Feedback Control: Analysis and Design*. New York: Wiley; 2007
- [8] Kwakernaak H. Robust control and H^∞ -optimization—Tutorial paper. *Automatica*. 1993;**29**(2):255-273
- [9] Zhou K, Doyle JC, Glover K. *Robust and Optimal Control*. New Jersey: Prentice Hall; 1996
- [10] Friedman J, Hastie T, Tibshirani R. *The Elements of Statistical Learning: Springer Series in Statistics*. New York: Springer; 2001
- [11] Soloway D, Haley PJ, editors. *Neural generalized predictive control*. In: *Proceedings of the 1996 IEEE International Symposium on Intelligent Control*; Dearborn: IEEE; 1996
- [12] Hecht-Nielsen R. Theory of the backpropagation neural network. In: *Neural Networks for Perception*. Cambridge, Massachusetts: Academic Press; 1992. pp. 65-93
- [13] Psaltis D, Sideris A, Yamamura AA. A multilayered neural network controller. *IEEE Control Systems Magazine*. 1988;**8**(2):17-21
- [14] Horng J-H. Hybrid MATLAB and LabVIEW with neural network to implement a SCADA system of AC servo motor. *Advances in Engineering Software*. 2008;**39**(3):149-155